CYP199A4 Supplementary data

Table S1. Sequence similarities and alignment between the Class I CYP systems from *R. palustris* HaA2 and *R. palustris* CGA009.

CYP199A4/HaPux/HaPuR	**CYP199A2/Pux/PuR**		
	Identities	Positives	Gaps
CYP199A4	356/412 (86%)	383/412 (92%)	2/412 (0%)
HaPux	74/106 (69%)	91/106 (85%)	1/106 (0%)
HaPuR	357/405 (88%)	374/405 (92%)	0/405 (0%)

Table S2. Spectral properties of CYP199A2, HaPux and HaPuR from *R. palustris* HaA2.

	Absorbance (nm)	**ε (mM^{-1} cm^{-1})**
CYP199A4	279	48.6
	357	27.9
	419	103.1
	538	9.4
	569	10.7
HaPux	280	18.7
	316	14.1
	416	11.2
	457	9.1
HaPuR	172	65.3
	383	9.6
	455	10.0
	482	8.2

Figure S1. Sequence alignment of HaPuR, PuR and PdR from *R. palustris* HaA2, *R. palustris* CGA009 and *P. putida* respectively.

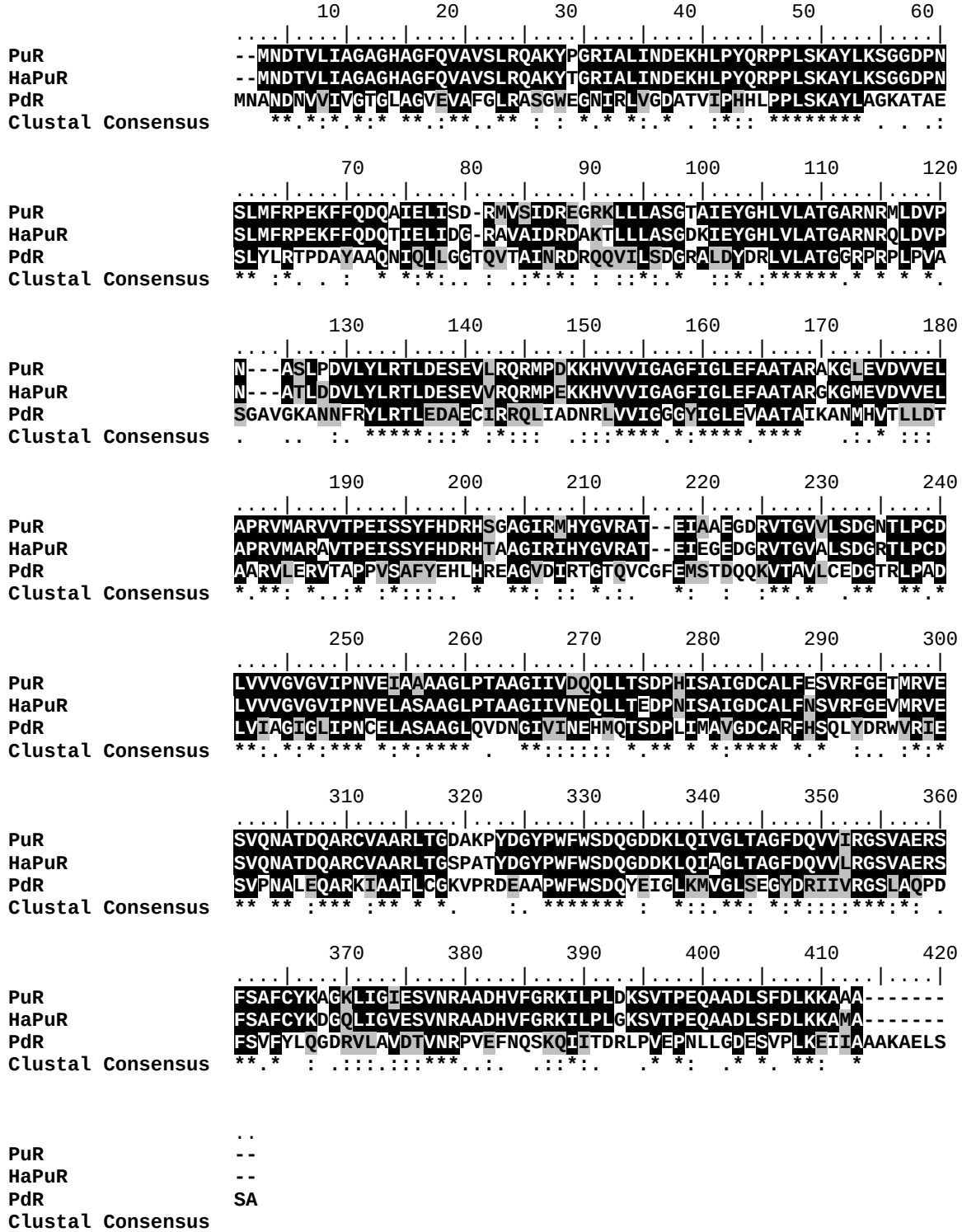

Figure S2. Sequence alignment of HaPux, Pux and Pdx from *R. palustris* HaA2, *R. palustris* CGA009 and *P. putida* respectively.

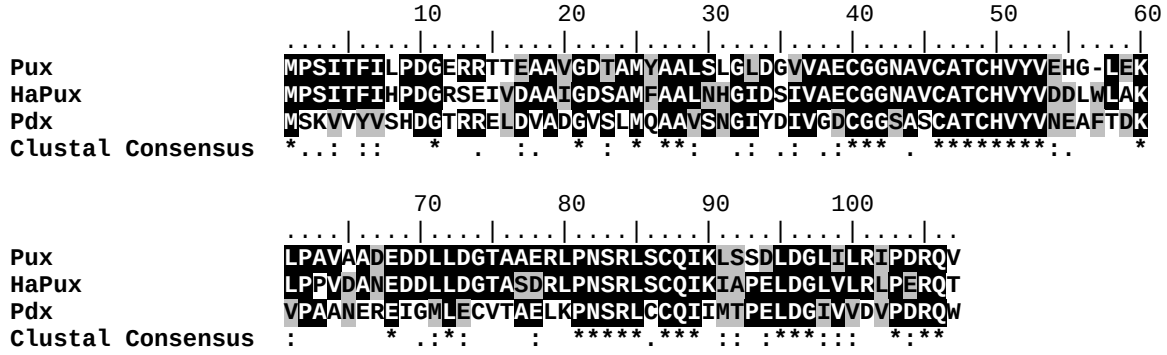

Figure S3. Sequence alignment of CYP199A4, CYP199A2 and CYP101A1 from *R. palustris* HaA2, *R. palustris* CGA009 and *P. putida* respectively.

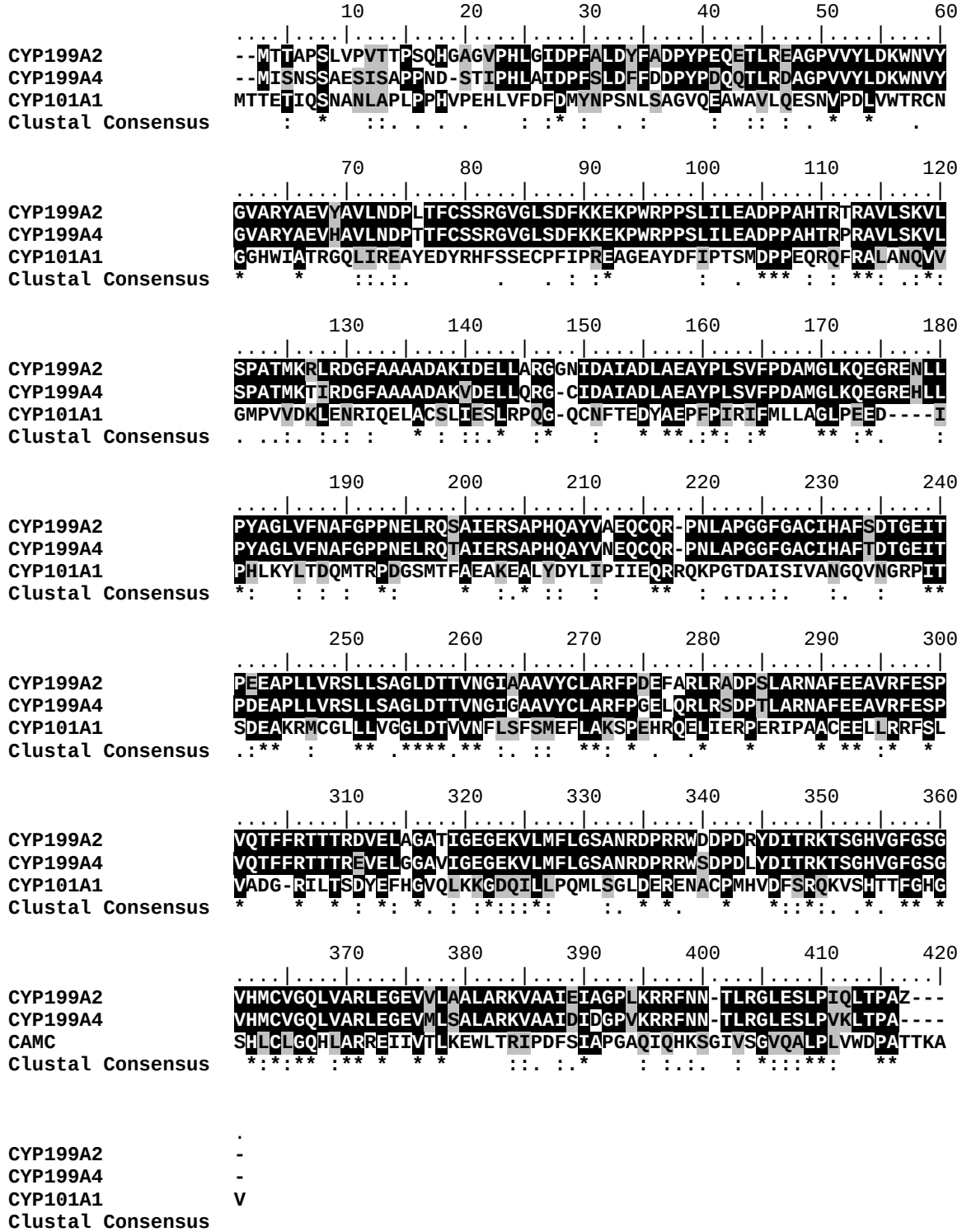

Figure S4. Electrospray mass spectra of (a) HaPuR (b) HaPux and (c) CYP199A4.

(a)

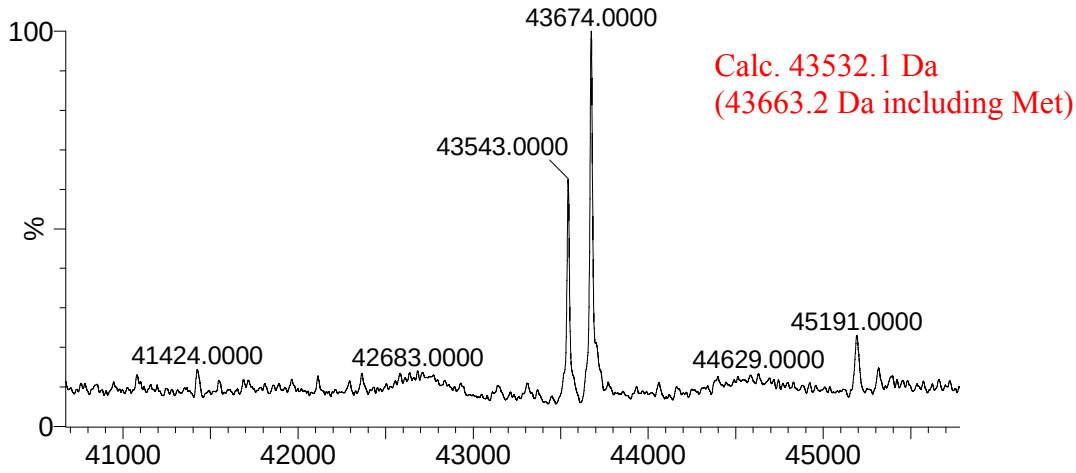

(b)

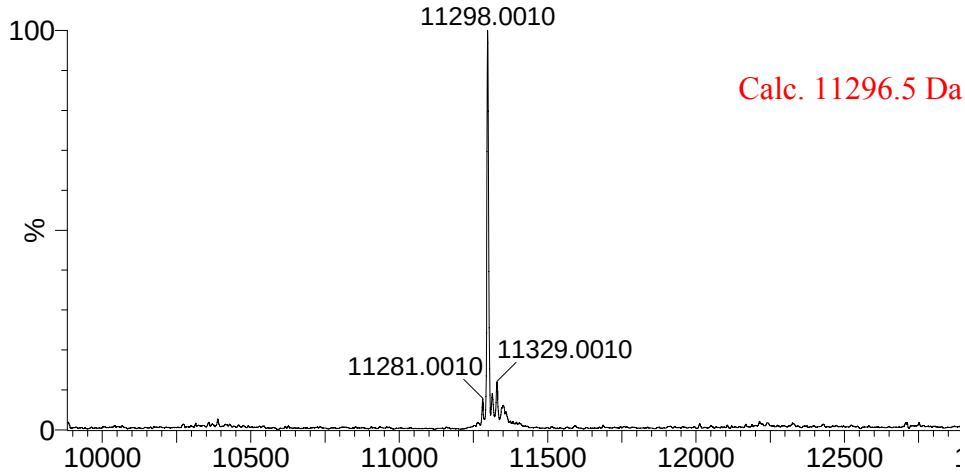

(c)

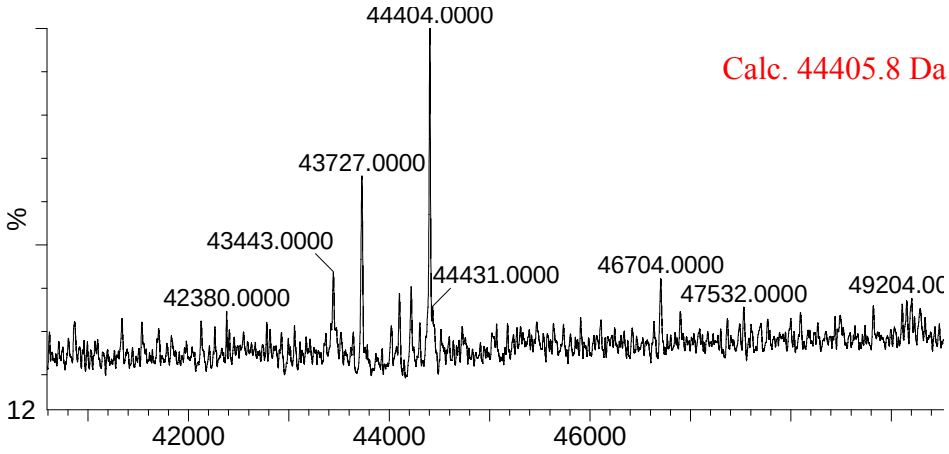

Figure S5. Construction of the plasmids of the whole cell oxidation system.

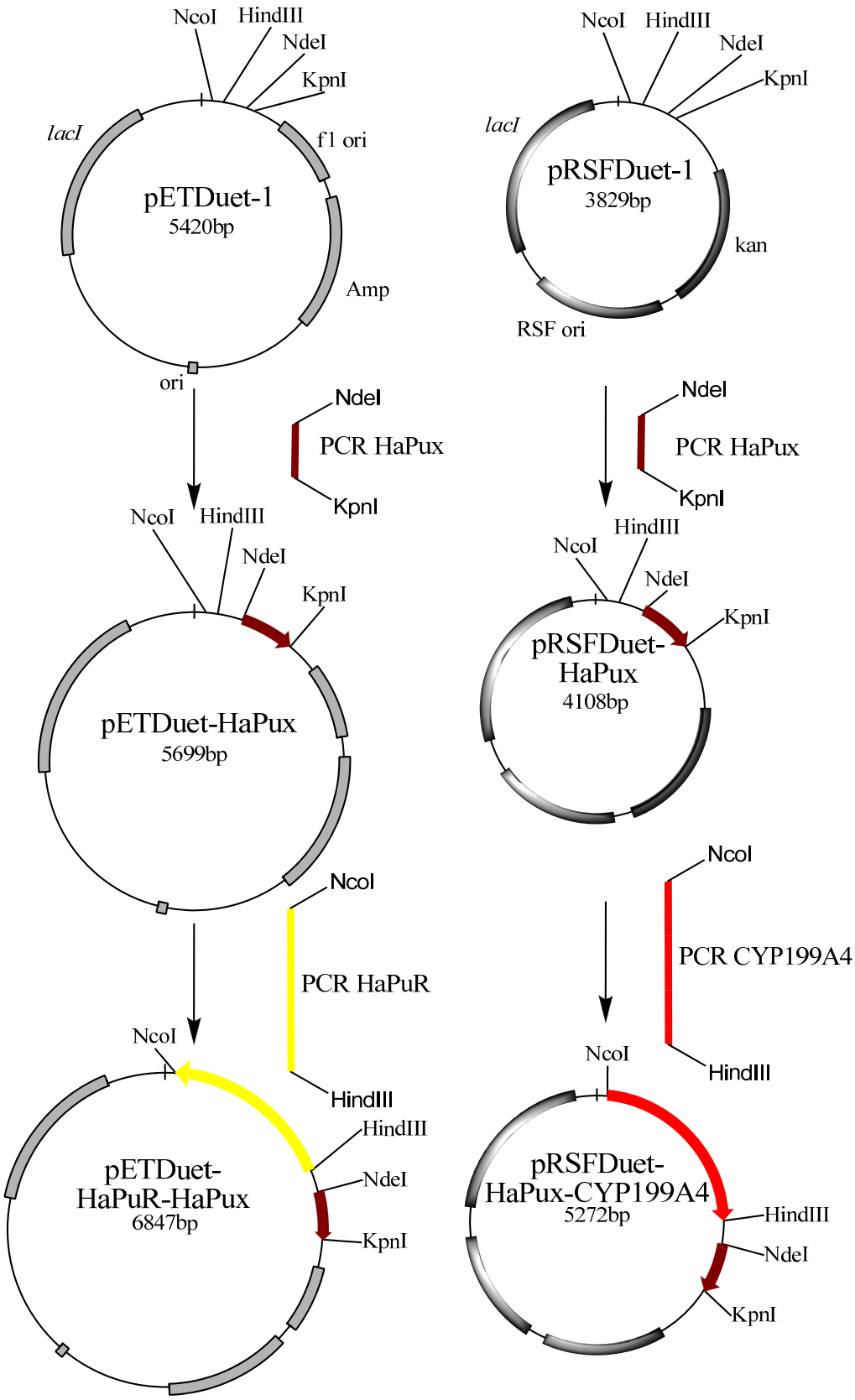

Figure S6. Example of NADH turnover data using CYP199A4 (0.5 μM), HaPux and HaPuR in a 1:10:1 ratio.